Mass Flow Rate of R-410A through Short Tubes Working near the Critical Point

Yongchan Kim[a], Vance Payne[b*], Jongmin Choi[c], Piotr Domanski[b]

[a]Department of Mechanical Engineering, Korea University
Anam-Dong, Sungbuk-Gu, Seoul, 136-701, KOREA
[b]Building Environment Division: HVAC&R Equipment Performance Group, NIST
100 Bureau Dr., MS 8631, Gaithersburg, MD 20899, USA
[c]Department of Mechanical Engineering, Hanbat National University
Duckmyung-Dong, Yusung-Gu, Daejeon, 305-719, KOREA

Abstract

Experimental data were taken to examine R-410A mass flow rate characteristics through short tube restrictors at upstream pressures approaching the critical point. Four short tube restrictors were tested by varying upstream pressure from 2619 kPa to 4551 kPa (corresponding to saturation temperature from 43.9 ^{o}C to 71.7 ^{o}C), upstream subcooling from 2.8 ^{o}C and 11.1 ^{o}C, and downstream pressure from 772 kPa to 1274 kPa. The experimental data were represented as a function of major operating parameters and short tube diameter. As compared to mass flow trends at typical upstream pressures, flow dependency on upstream subcooling was more significant at high upstream pressures due to a higher density change. Based on the database obtained from this study and literature, an empirical correlation was developed from a power law form of dimensionless parameters generated by the Buckingham Pi theorem. The post-predictions of the new correlation yielded average and mean deviations of 0.11 % and 2.4 %, respectively.

**Corresponding author. Tel.: +(301) 975-6663; fax (301) 975-8973*
E-mail address: vance.payne@nist.gov

Keywords: Air conditioning, critical point, mass flow rate, R-410A, short tube restrictor

Nomenclature

a	Exponents of Pi-groups
D	Inner diameter (m)
L	Length (m)
$\dot{m}$	Mass flow rate (kg/s)
P_c	Critical pressure (kPa)
P_{up}	Upstream pressure (kPa)
P_{sat}	Saturated pressure (kPa)
T_c	Critical temperature (°C)
ΔT_{sub}	Degree of subcooling (°C)

Greek letters

ρ	Density (kg/m^3)
π	Dimensionless parameter group
μ	Viscosity (Pa•s)

Subscripts

f	Saturated liquid
g	Saturated vapor
meas	Measured
pred	Predicted

1. Introduction

R-410A has become the leading R-22 replacement for unitary air conditioners and heat pumps. The efficiency of an R-410A air conditioner at standard rating conditions is comparable to that of an R-22 system. However, the performance at elevated ambient temperatures deteriorates faster for the R-410A system than for its R-22 counterpart [1,2,3]. This is because the critical temperature of R-410A (72.03 °C) is lower than that of R-22 (96.2 °C), and thermodynamic irreversibilities are more severe as the cycle approaches the critical point of the refrigerant. Since a loss of subcooling at the inlet to the expansion device promotes efficiency degradation, it is of particular interest to understand R-410A flow characteristics for the complete range of operating conditions, including the upstream pressure region corresponding to high ambient temperatures.

A short tube restrictor has been widely utilized as an expansion device in residential air-conditioners and heat pumps because of its low cost, high reliability, ease of installation, and elimination of additional check valves used for flow direction change in heat pump applications [4,5,6]. During the past few decades, many researchers have extensively investigated the performance of short tube restrictors. Early studies on two-phase flow through short tube restrictors focused exclusively on R-12 and R-22 [4,7,8,9,10]. Aaron and Domanski [4] presented experimental data and an empirical correlation for R-22 flowing through short tube restrictors at subcooled inlet conditions. Their correlation was developed by modifying the single-phase orifice equation based on their test data for R-22. Kim and O'Neal [10] also presented an empirical flow correlation for short tube restrictors using R-22 by extending the Aaron and Domanski correlation [4]. Recently, several researchers presented the performance of short tube restrictors using alternative refrigerants [5,6,11]. Kim and O'Neal [5] analyzed the performance of short tube restrictors and developed a two-phase flow model for R-134a by modifying the single-phase orifice equation. Payne and

O'Neal [11] also developed a flow model for R-407C and R-410A in a similar format to the Kim and O'Neal correlation [5] based on an extensive database. Payne [6] developed a universal correlation for R-12, R-134a, R-502, R-22, R-407C, and R-410A flowing through short tube restrictors at subcooled and two-phase inlet conditions by correlating dimensionless parameters.

Most R-410A mass flow data and correlations were obtained at typical condensing temperatures, ranging from 35 ^{o}C to 54 ^{o}C [6, 11], and data for high condensing temperatures (high upstream refrigerant pressures) are very limited even though the R-410A system sometimes operates near the critical point due to an elevated ambient temperature [1]. Therefore, the analysis and correlation for the performance of short tube restrictors working near the critical point of R-410A are needed to facilitate short tube selection. The objective of this study was to obtain experimental data for R-410A for high upstream pressures, which would extend the data collected by Payne and O'Neal [11] to the subcritical region and allow the development of a new empirical correlation for a wide range of operating pressures from typical to near the critical point.

2. Experimental setup

The experimental setup used in this study was designed to control upstream pressure, upstream subcooling, and downstream pressure of a short tube restrictor. As shown in Fig. 1, the test setup consists of a compressor, a condenser, a subcooler, a tape heater, a detachable test section, an evaporator, and an oil separator. The compressor was customized for testing at higher outdoor temperatures by installing a powerful electric motor. The oil separator was installed between the outlet and inlet of the compressor to minimize the effects of oil on the flow rate through the short tube restrictors. The condensing unit, including the compressor and a fin-tube type condenser, was installed in an outdoor chamber to control

upstream pressure by adjusting outdoor temperature. The refrigerant subcooling entering the test section was set by varying the flow rate of cold water to the subcooler and adjusting the electric power input to the tube heater. The two-phase refrigerant exiting the test section was evaporated in the plate type evaporator. The downstream pressure of the test section was controlled by adjusting the temperature and flow rate of the hot water.

Short tube restrictors and test conditions used in this study are listed in Table 1. The diameters of the tested short tube restrictors range from 1.10 mm to 1.80 mm with a fixed length of 12.70 mm. A series of tests for each test section was run to investigate the influence of the operating parameters on the mass flow rate though the short tube restrictor. The test matrix was chosen to cover a wide range of operating conditions for a short tube restrictor found in a typical residential heat pump or air-conditioner using R-410A at high ambient temperatures. The upstream pressure was varied from 2619 kPa to 4551 kPa, corresponding to saturation temperature from 43.9 ^{o}C to 71.7 ^{o}C, while the downstream pressure was set at 772 kPa, 918 kPa, 1085 kPa, and 1274 kPa. The upstream subcooling was varied between 2.8 ^{o}C and 11.1 ^{o}C. Oil concentration was measured at the outlet of the subcooler according to ASHRAE STANDARD 41.1 [12]. During the experiments, the measured oil concentration was less than 0.3 %, which showed negligible effects on mass flow rate through the short tube restrictors [6].

The length of a short tube restrictor was measured by a dial caliper with an uncertainty of ± 0.001 mm. The short tube diameter was measured using a precision plug gauge set with an uncertainty of ± 0.001 mm. The pressures and temperatures of the refrigerant at the inlet and outlet of the test section were monitored using pressure transducers with an uncertainty of ± 2.1 kPa and T-type thermocouples with an uncertainty of ± 0.2 °C, respectively. The refrigerant flow rate was measured in the liquid line between the subcooler and the tape heater using a Coriolis effect flow meter with an uncertainty of ± 0.2%

of the reading. The data were recorded every 5 s and averaged for a period of 4 minutes after steady state conditions were reached. All stated uncertainties are for the standard uncertainty with a coverage factor of 2.0.

3. Experimental results and discussion

Fig. 2 shows the mass flow rate with respect to upstream subcooling at two upstream pressures and three tube diameters. The mass flow rates increase linearly with subcooling. However, the slope of mass flow rate as a function of subcooling is greater for the higher upstream pressure, and the difference in slopes is greater for larger diameters. For an increase in subcooling of 2.8 ^{o}C to 11.1 ^{o}C, the average mass flow rate increase is 27.9 % for an upstream pressure of 2619 kPa and 37.5 % for an upstream pressure of 4327 kPa. Refrigerant subcooling affects the mass flow rate through the inlet refrigerant density and the location of the flash point in the tube, which is related to the available subcooled liquid pressure drop (the pressure difference between upstream pressure and saturated liquid pressure corresponding to the inlet temperature). As subcooling decreases, the subcooled liquid pressure drop decreases and the flashing point moves toward the inlet of the short tube [13], which reduces the mass flow. Also, a decrease in subcooling reduces the mass flow rate through a decrease in inlet density. For example, a decrease of subcooling from 11.1 ^{o}C to 2.8 ^{o}C, reduces the upstream densities by 4.7 % and 9.7 % for upstream pressures of 2619 kPa and 4327 kPa, respectively. The stronger effect on the density at the higher pressure indicates that the influence of subcooling on mass flow rate is more significant in proximity to the critical point.

Fig. 3 shows mass flow rate with respect to upstream pressure at different subcooling levels. As upstream pressure increases, the mass flow rate linearly increases for all subcooling levels even though upstream pressure is as high as 4551 kPa corresponding to a

saturation temperature of 71.7 ^{o}C. The slope of mass flow rate as a function of upstream pressure gradually increases with a rise of subcooling from 2.8 ^{o}C to 5.6 ^{o}C, while it remains nearly constant with an increase of subcooling from 5.6 ^{o}C to 11.1 ^{o}C. It was also observed that the R-410A system became unstable when the subcooling was lower than 2.8 ^{o}C at high upstream pressures. This would suggest that the subcooling of the R-410A air conditioner working at high ambient temperatures (corresponding to high upstream pressures) should be higher than 5.6 ^{o}C to exclude the possibility of severe reduction of mass flow rate and "hunting" effects.

Fig. 4 shows the present data and the data obtained by Payne and O'Neal [11] for R-410A for two diameter tubes. The experimental results obtained from the two studies are very consistent with each other. The figure shows a linear relation between the upstream pressure and mass flow rate for a given level of subcooling, with the slope of mass flow rate as a function of upstream pressure increasing with subcooling for the larger diameter short tube. As shown in Fig. 4, when increasing the short tube diameter from 1.097 mm to 1.717 mm, the slope increases by 67 % and 74 % at subcooling levels of 5.6 ^{o}C and 11.1 ^{o}C, respectively. Therefore, a large-diameter short tube employed in the R-410A system operating at high ambient temperatures will experience a more severe reduction of mass flow rate when upstream subcooling decreases.

Fig. 5 shows mass flow rate with respect to short tube diameter for three upstream pressures. The mass flow rate is proportional to $D^{2.2}$, which is consistent with the previous results for R-22, R-134a, and R-410A at the typical operating pressure range [4,6,13]. Aaron and Domanski [4] and Kim [13] showed that the mass flow rate was approximately proportional to D^{2}. As short tube diameter increases from 1.097 mm to 1.803 mm at an upstream pressure of 4327 kPa, the mass flow rate increases by 199 % from 92.9 kg/h to 278 kg/h. The slope of the mass flow rate curve with respect to short tube diameter slightly

increases with a rise of upstream pressure.

4. Development of an empirical correlation

The database used for the development of the correlation consists of the measurements obtained under the current study and those obtained by Payne and O'Neal [11]. The database contains a total of 210 data points. The database covers short tube diameters from 1.0 mm to 2.0 mm, short tube lengths from 12.7 mm to 25.4 mm, upstream pressures from 2130 kPa to 4551 kPa, downstream pressures from 420 kPa to 1500 kPa, and inlet subcoolings from 0 ^{o}C to 11.1 ^{o}C. All short tube restrictors included in the database have a sharp-edged entrance shape and were attached to a tube with inner diameter of approximately 8.0 mm.

The parameters influencing mass flow rate through short tube restrictors are selected and modified based on the data analysis. Operating parameters considered in this study are upstream pressure, P_{up}, and upstream subcooling, ΔT_{sub}. Downstream pressure, P_{down}, is not included because choking is easily established in short tube restrictors for typical steady-state applications. The inlet temperature and pressure are used to calculate the subcooled liquid pressure difference, $P_{up} - P_{sat}$, to consider the effect of subcooled liquid pressure drop, which shows strong influence on mass flow rate through short tube restrictors [4,13]. Among refrigerant properties, viscosity, μ, and density, ρ, of both the liquid and vapor phases are considered in the correlation. In addition to these variables, the critical temperature, T_c, is also included to non-dimensionalize upstream subcooling, ΔT_{sub}. Short tube diameter, D, and length, L, are included to consider geometric effects on mass flow rate. The resulting relationship between the mass flow rate and the selected variables has the following functional form:

$$\dot{m} = f((P_{up} - P_{sat}), \Delta T_{sub}, L, D, \mu_f, \mu_g, \rho_f, \rho_g, T_c) \quad (1)$$

Six dimensionless Pi-groups are derived from applying the Buckingham Pi theorem [14] to the variables in Eq (1) with the four repeating variables of D, ρ_f, μ_f, and T_c. The definitions and effects of each Pi-group (π_1 through π_6) are given in Table 2. To generate a simple form of dimensionless Pi-groups, the complicated repeating variable $\mu_f^2/(\rho_f D^2)$ included in π_2 is replaced by critical pressure, P_c, in the modified parameter. Therefore, the redefined π_2 becomes $(P_{up} - P_{sat})/P_c$, which indicates subcooled liquid pressure drop. In addition, the original π_6 group, μ_g/μ_f, is replaced by $(\mu_f - \mu_g)/\mu_g$ since the modified parameter shows better dependence on mass flow rate. The vapor to liquid density ratio, π_5, can be used as an indicator of the slip ratio between phases at the short tube exit plane [15].

The correlation for the dimensionless mass flow rate, π_1, is generated in a power law form of the remaining Pi-groups.

$$\pi_1 = \mathrm{a}_1 \, \pi_2^{a_2} \, \pi_3^{a_3} \, \pi_4^{a_4} \, \pi_5^{a_5} \, \pi_6^{a_6} \qquad (2)$$

The coefficient a_1 and exponents of the five independent Pi-groups were determined using a non-linear regression. All refrigerant properties were calculated using REFPROP [16]. The obtained correlation has the following final form:

$$\pi_1 = 0.80255 \, \pi_2^{3.0949} \, \pi_3^{-3.1066} \, \pi_4^{-0.1904} \, \pi_5^{-2.6183} \, \pi_6^{-1.4843} \qquad (3)$$

5. Comparison of the correlation

Fig. 6 shows the comparison of the post-predicted mass flow rates with the database. The correlation yields good agreement with the measured data with an average deviation of 0.11 % and a mean deviation of 2.4 % (defined in Table 3). Approximately 92 % of the present database is correlated within a relative deviation of ± 5 %. Most large deviations

occur at low flow rates due to higher experimental uncertainties in the low flow range.

To compare the application limits of the correlation, the predicted mass flow rates using the present correlation are compared with the existing correlations developed by Payne [6] and Payne and O'Neal [11]. Figs. 7 and 8 show relative deviations of the predictions using the correlations of this study, Payne [6], and Payne and O'Neal [11] based on the present database at typical (2130 - 3180 kPa) and high (3180 - 4551 kPa) upstream pressures, respectively. For upstream pressures from 2130 kPa to 3180 kPa, relative deviations of the present correlation are from -8.3 % to +11.8 %, while those for the Payne correlation, and the Payne and O'Neal correlation are from -8.4 % to +19.5 % and from -4.4 % to +22.6 %, respectively. For upstream pressures from 3180 kPa to 4551 kPa, the present correlation yields relative deviations from -4.1 % to +5.9 %, while the Payne correlation, and the Payne and O'Neal correlation predict the data with relative deviations from –14.3 % to +24.7 % and from -2.7 % to +14.7 %, respectively.

Table 3 shows average and mean deviations of the correlations of this study, Payne [6], and Payne and O'Neal [11] from the present database. The Payne correlation [6] shows good predictions at upstream pressures from 2100 kPa to 3000 kPa with average and mean deviations of 2.98 % and 3.98 %, respectively. However, it yields large deviations at upstream pressures from 4000 kPa to 4700 kPa with average and mean deviations of 1.68 % and 10.92 %, respectively. The Payne and O'Neal correlation [11] yields satisfactory predictions with average and standard deviations of 1.08 % and 3.67 %, respectively. However, their correlation shows some over-predictions at high upstream pressures due to limitations in the range of their database. Based on these comparisons, it can be concluded that the proposed dimensionless-parameter-based correlation is appropriate for use over a wide range of upstream pressures from typical upstream pressures to those near the critical point.

5. Conclusions

The mass flow rates of R-410A flowing through short tube restrictors were measured at typical (2130 kPa - 3180 kPa) and high (3180 kPa - 4551 kPa) upstream pressures. The mass flow rates are strongly dependent on upstream pressure, upstream subcooling, and short tube diameter, which is very similar to the trends observed at typical upstream pressures. However, the decrease of mass flow rate with a reduction of subcooling becomes more significant when upstream pressure increases beyond 3604 kPa due to a higher density change. The positive relationship between mass flow rate and upstream pressure becomes weaker with a reduction of subcooling and a decrease of short tube diameter. Based on the database obtained from this study and the literature, an empirical correlation for predicting mass flow rate of R-410A through short tube restrictors was developed from a power law form of dimensionless parameters, which are generated by the Buckingham Pi theorem considering the effects of short tube inlet conditions, short tube geometries, and refrigerant properties. The present correlation agrees with the measured data with an average deviation of 0.11 % and a mean deviation of 2.4 %. Approximately 92 % of the experimental data used in this study are correlated within a relative deviation of ± 5 %.

Acknowledgements

This study was supported by the National Institute of Standards and Technology, Gaithersburg, MD, USA, and the Korea University, Seoul, Korea.

References

[1] Motta SY, Domanski PA, Performance of R-22 and its alternatives working at high outdoor temperatures. In: The Eighth International Refrigeration Conference, IN, USA, 2000.

[2] Wells W, Bivens D, Yokozeki A, Rice CK, Air conditioning system performance with R-410A at high ambient temperatures, In: Presentation at Seminar on Alternative Refrigerants for Unitary Heat Pumps and Air Conditioners, ASHRAE Annual Meeting, Seattle, WA, 1999.

[3] Domanski PA, Payne WV, Properties and cycle performance of refrigerant blends operating near and above the refrigerant critical point. Air-Conditioning and Refrigeration Technology Institute Final Report, ARTI-21CR/50010-02, Virginia, USA, 2002.

[4] Aaron AA, Domanski PA, Experimentation, analysis, and correlation of refrigerant-22 flow through short tube restrictors. ASHRAE Transactions 1990; 96(1): 729-742.

[5] Kim Y, O'Neal DL, A semi-empirical model of two-phase flow of refrigerant-134a through short tube orifices. Experimental Thermal and Fluid Science 1994; 9:426-435.

[6] Payne WV, A universal mass flow rate correlation for refrigerants and refrigerant/oil mixtures flowing through short tube orifices. Ph.D Thesis, Texas A&M University, Texas, USA, 1997.

[7] Pasqua PF, Metastable flow of Freon-12. Refrigeration Engineering 1953; 61:1084-1088.

[8] Mei VC, Short tube refrigerant restrictors. ASHRAE Transactions 1982; 88(2): 157-168.

[9] Krakow KI, Lin S, Refrigerant flow through orifices. ASHRAE Transactions 1988; 94(1): 484-506.

[10] Kim Y, O'Neal DL, Two-phase flow of refrigerant-22 through short tube orifices. ASHRAE Transactions 1993; 100(1): 323-334.

[11] Payne WV, O'Neal DL, Two-phase flow of two HFC refrigerant mixtures through short tube orifices. U.S. Environmental Protection Agency, Report-600/R-95-168, 1995.

[12] ASHRAE, Standard method for measurement of proportion of oil in liquid refrigerant.

ANSI/ASHRAE Standard 41.4, American Society of Heating, Refrigerating, and Air-Conditioning Engineers, Inc. Atlanta, USA, 1984.

[13] Kim Y, Two-phase flow of HCFC-22 and HFC-134a through short tube orifices. Ph.D Thesis, Texas A&M University, Texas, USA, 1993.

[14] White FM, Fluid Mechanics. 2nd Ed., NY: McGraw-Hill Inc. 1986.

[15] Wallis GB, Critical two-phase flow. International Journal of Multiphase Flow 1980; 6: 97-112.

[16] McLinden MO, Klein SA, Lemmon EW, Peskin AP. NIST thermodynamic and transport properties of refrigerant and refrigerant mixtures (REFPROP). Version 6.01. Gaithersburg, MD: NIST, 1998.

Table 1 Short tube restrictors and test conditions

Short tube restrictor geometry	Length (mm)	12.7
	Diameter (mm)	1.10, 1.34, 1.72, 1.80
Operating conditions	Upstream pressure (kPa)	2619, 3180, 3604, 3833, 4327, 4551
	Upstream subcooling (°C)	2.8, 5.6, 11.1
	Downstream pressure (kPa)	772, 918, 1085, 1274

Table 2 Dimensionless Pi-groups

Pi-group	Original parameter	Modified parameter	Effects
π_1	$\frac{\dot{m}}{D\mu_f}$	$\frac{\dot{m}}{D^2\sqrt{\rho_f P_{up}}}$	Flow rate
π_2	$\frac{(P_{up}-P_{sat})\rho_f D^2}{\mu_f{}^2}$	$\frac{P_{up}-P_{sat}}{P_c}$	Upstream pressure
π_3	$\frac{\Delta T_{sub}}{T_c}$	$\frac{\Delta T_{sub}}{T_c}$	Subcooling
π_4	$\frac{L}{D}$	$\frac{L}{D}$	Geometry
π_5	$\frac{\rho_g}{\rho_f}$	$\frac{\rho_g}{\rho_f}$	Density
π_6	$\frac{\mu_g}{\mu_f}$	$\frac{\mu_f-\mu_g}{\mu_g}$	Viscosity

Table 3 Comparison of the correlations with experimental data

Correlations		Data source: Present, Payne and O'Neal [11]			
		Upstream pressure (kPa)			
		2100 to 3000	3000 to 4000	4000 to 4700	All ranges
Payne [6]	Ave. dev.*	2.98	1.21	1.68	2.22
	Mean. dev.**	3.98	5.21	10.92	5.12
Payne and O'Neal [11]	Ave. dev.*	0.83	0.86	2.87	1.08
	Mean. dev.**	2.50	1.74	3.23	2.32
Present study	Ave. dev.*	0.18	0.20	-0.43	0.11
	Mean. dev.**	2.75	0.20	2.33	2.40

* $\text{Ave. dev.} = \frac{1}{n}\sum_{1}^{n}[(\dot{m}_{pred} - \dot{m}_{meas}) \times 100) / \dot{m}_{meas}]$

** $\text{Mean. dev.} = \frac{1}{n}\sum_{1}^{n}[|\dot{m}_{pred} - \dot{m}_{meas}| \times 100) / \dot{m}_{meas}]$

Figure captions

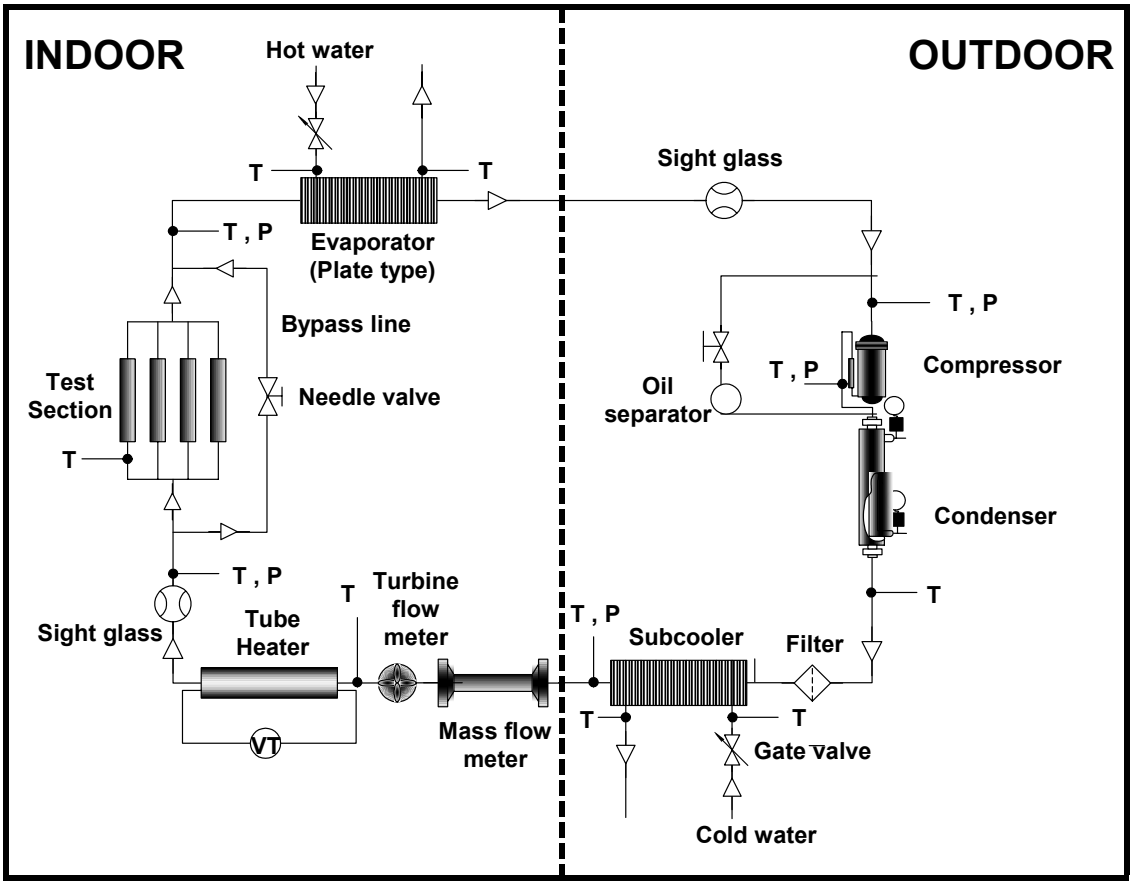

Fig. 1 Schematic diagram of the experimental setup.

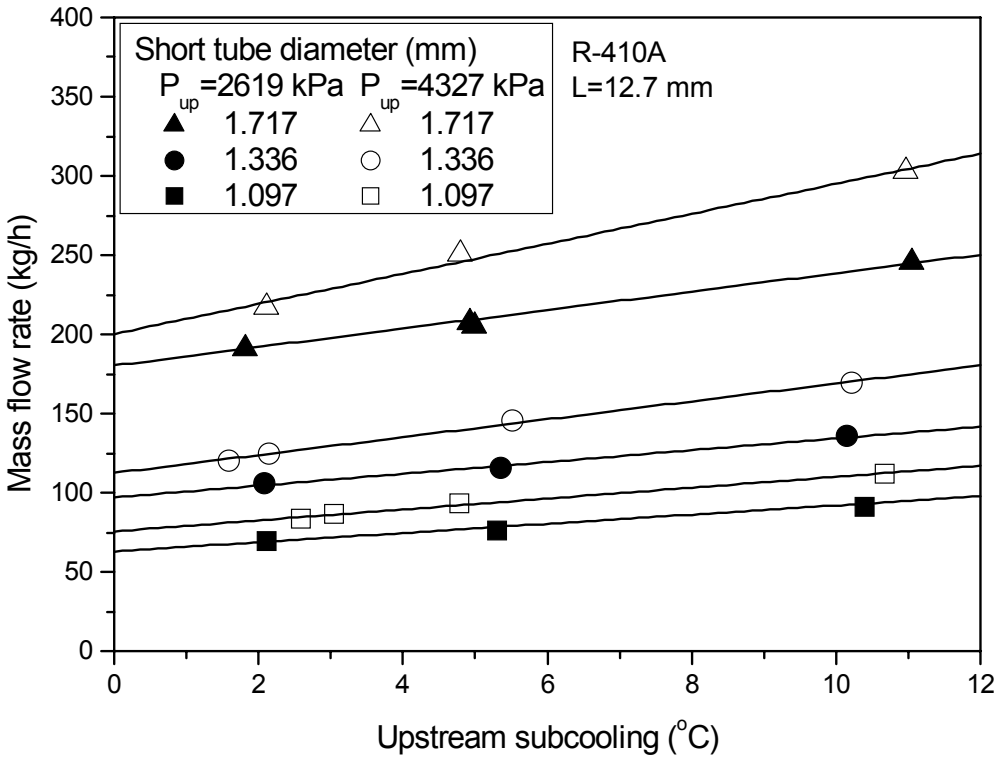

Fig. 2 Mass flow rate with respect to upstream subcooling for different short tube diameters.

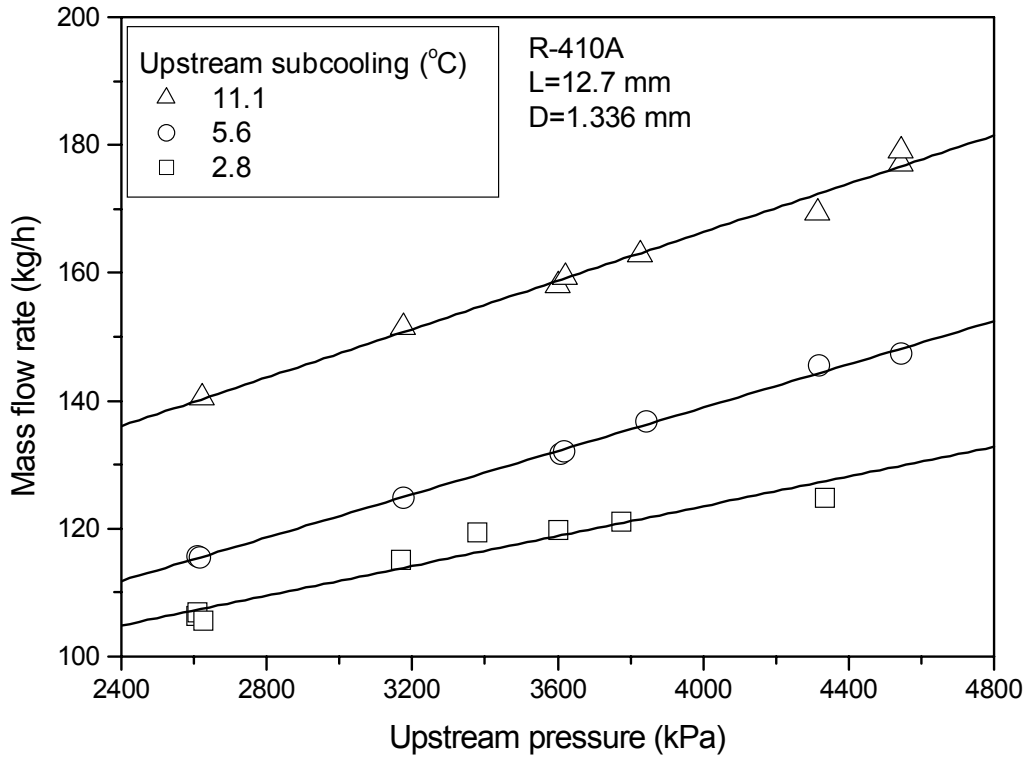

Fig. 3 Mass flow rate with respect to upstream pressure for different subcoolings.

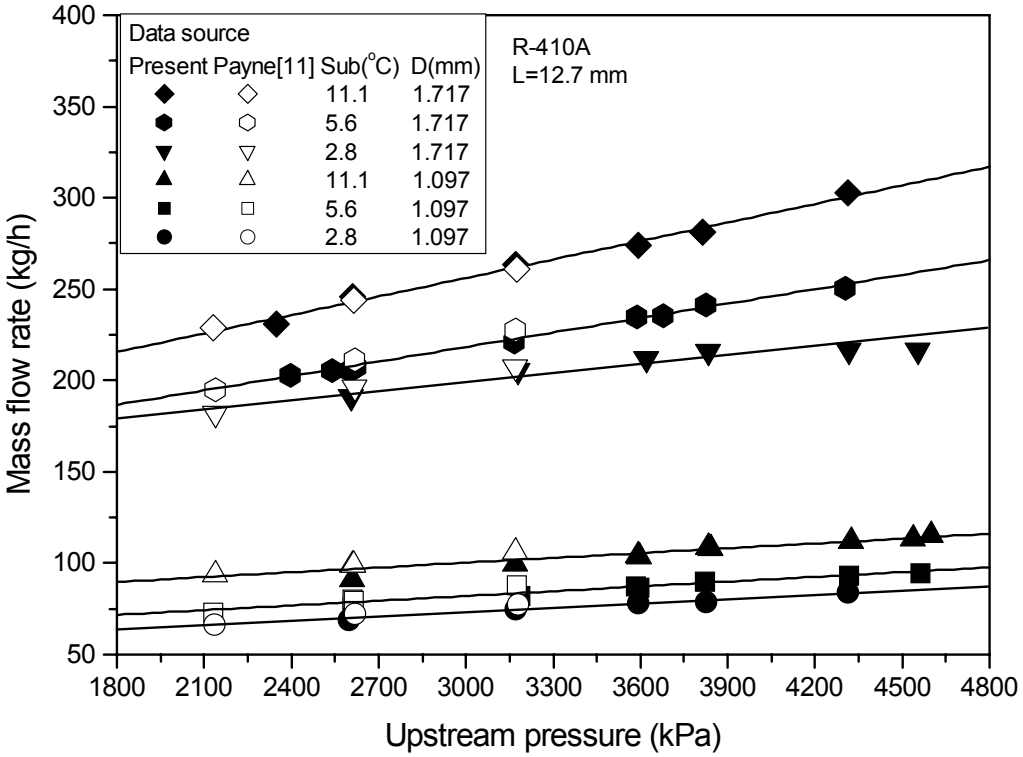

Fig. 4 Comparison of the present data with Payne and O'Neal's [11] for data extension over typical operating conditions.

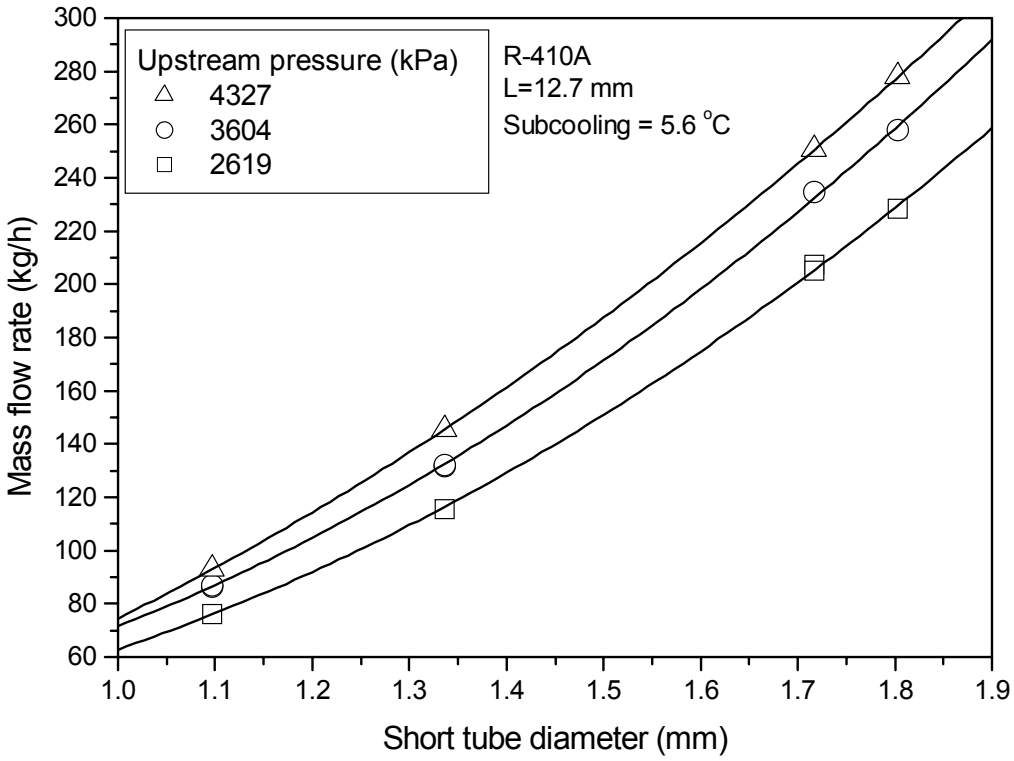

Fig. 5 Mass flow rate with respect to short tube diameter for different upstream pressures.

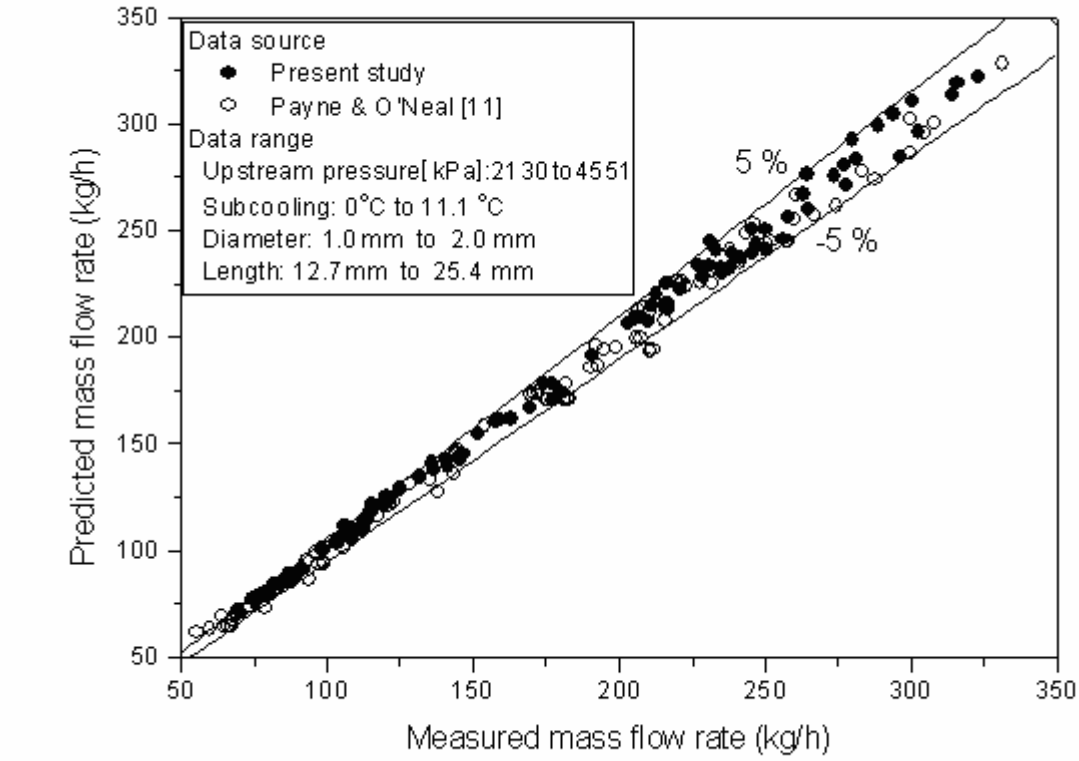

Fig. 6 Comparison of the present correlation's predictions with the database.

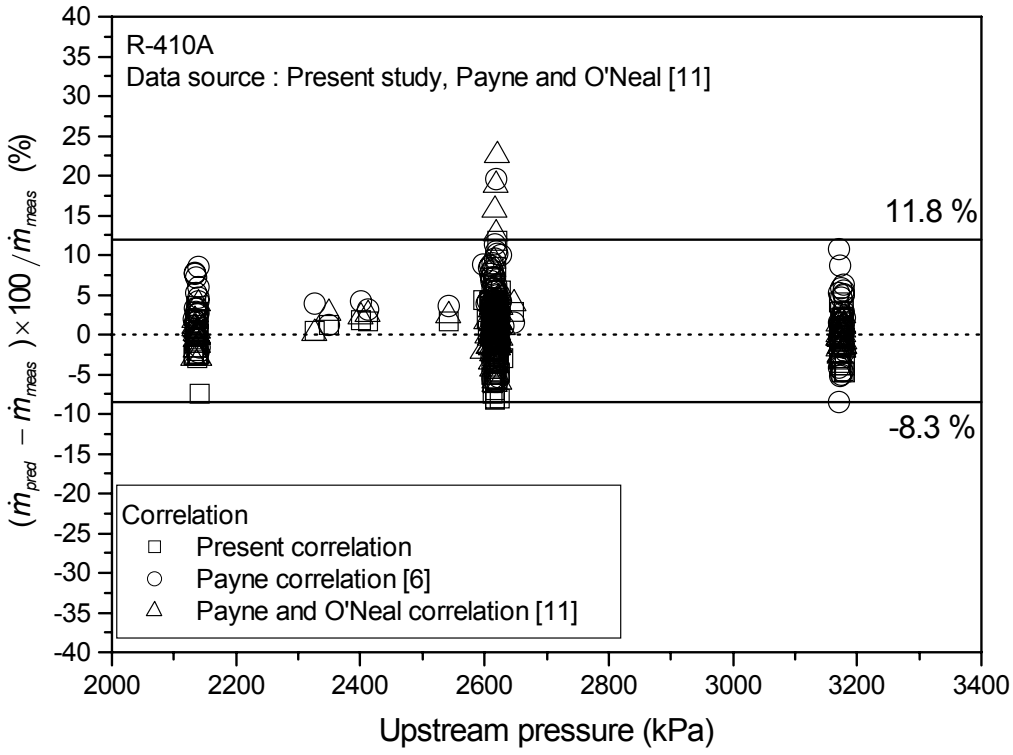

Fig. 7 Deviations of several correlations' predictions from measured data at upstream pressures from 2130 to 3180 kPa.

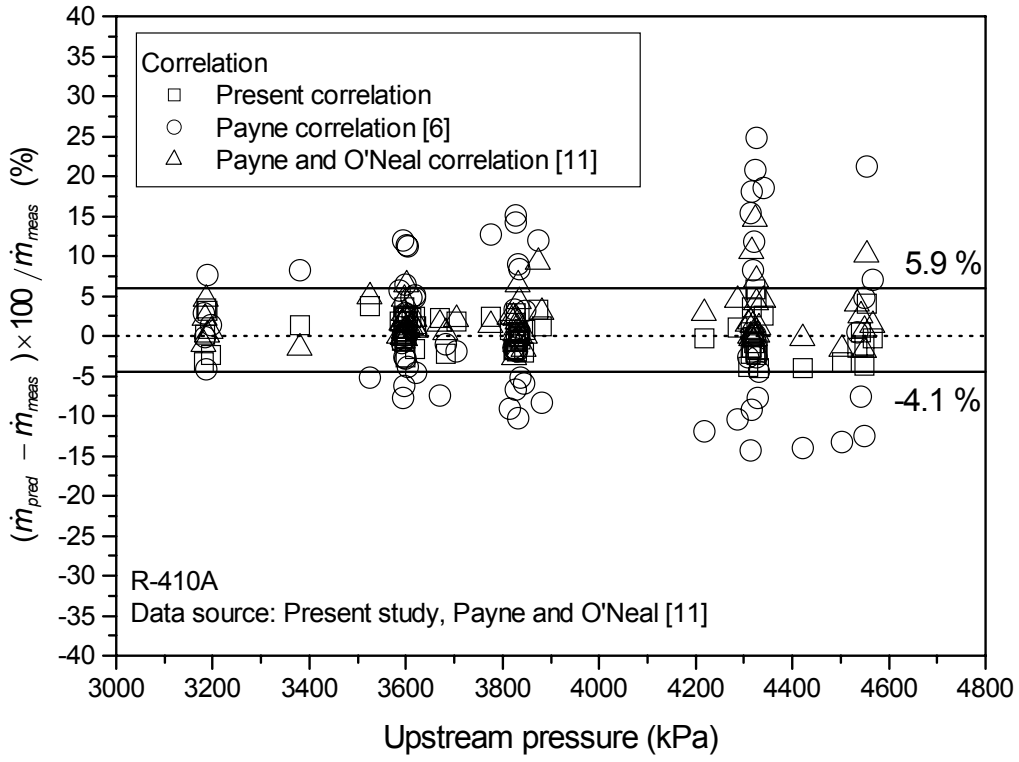

Fig. 8 Deviations of several correlations' predictions from measured data at upstream pressures from 3180 kPa to 4551 kPa.